

Mid-infrared interferometry of massive young stellar objects

H Linz¹, B Stecklum², R Follert^{1,2}, Th Henning¹, R van Boekel¹, A Men'shchikov³, I Pascucci⁴ and M Feldt¹

¹ MPIA Heidelberg, Königstuhl 17, D-69117 Heidelberg, Germany

² Thüringer Landessternwarte Tautenburg, Sternwarte 5, D-07778 Tautenburg, Germany

³ CEA, IRFU, Service d'Astrophysique, F-91191 Gif-sur-Yvette, France

⁴ Steward Observatory, Department of Astronomy, University of Arizona, 933 N Cherry Ave., Tucson AZ 85721-0065, U.S.A.

E-mail: [linz,follert,henning,boekel,mfeldt]@mpia.de, stecklum@tls-tautenburg.de, alexander.menshchikov@cea.fr, pascucci@as.arizona.edu

Abstract. The very inner structure of massive YSOs is difficult to trace. With conventional observational methods we identify structures still several hundreds of AU in size. However, the (proto-)stellar growth takes place at the innermost regions (<100 AU) where the actual mass transfer onto the forming high-mass star occurs. We present results from our programme toward massive YSOs at the VLTI, utilising the two-element interferometer MIDI. To date, we observed 10 well-known massive YSOs down to scales of 20 mas (typically corresponding to 20 - 40 AU for our targets) in the 8-13 micron region. We clearly resolve these objects which results in low visibilities and sizes in the order of 30-50 mas. For two objects, we show results of our modelling. We demonstrate that the MIDI data can reveal decisive structure information for massive YSOs. They are often pivotal in order to resolve ambiguities still immanent in model parameters derived from sole SED fitting.

1. Introduction

High-mass stars predominantly form in clustered environments much more distant than typical well-investigated low-mass star-forming regions. Thus, high spatial resolution is a prerequisite for making progress in the observational study of high-mass star formation. Furthermore, all pre-main sequence phases are usually deeply embedded. This often forces observers of embedded massive young stellar objects (MYSOs) to move to the mid-infrared (MIR) where the resolution of conventional imaging is limited to $> 0''.25$ even with 8-m class telescopes. Hence, one traces linear scales still several hundred AU in size even for the nearest MYSOs, and conclusions on the geometry of the innermost circumstellar material remain ambiguous. MIR emission moderately resolved with single telescopes may even arise from the inner outflow cones [3, 12].

A versatile method to overcome the diffraction limit of single telescopes is to employ interferometric techniques. We are conducting a larger survey toward MYSOs based on MIR interferometry. In total, we have observed 10 sources so far. All these sources, mostly comprising BN-type objects [5], are clearly resolved with the interferometer baselines we applied (≥ 16 m). This in itself is a major step forward compared to the previous more or less unresolved thermal infrared imaging with 4- to 8-m class telescopes for these sources.

2. Observations and Modelling

Visibilities in the mid-infrared wavelength range 8–13 μm have been obtained with the instrument MIDI [10] at the Very Large Telescope Interferometer. Within the framework of Guaranteed Time Observations for MIDI as well as Director’s Discretionary Time, we observed our objects at several 8.2-m Unit Telescope (UT) baseline length / baseline orientation combinations between June 2004 and May 2006. Additionally, first observations with the 1.8-m Auxiliary Telescopes (ATs) have been performed in autumn 2006 and spring 2007 for three of our sources.

We refer to [11] for a more detailed description of the standard observing procedure for MIDI observations. For all our observations, the so-called HighSens mode was used: during self-fringe tracking, all the incoming thermal infrared signal is used for beam combination and fringe tracking, while the photometry is subsequently obtained in separate observations. We use the MIDI prism as the dispersing element, hence, we finally get spectrally dispersed visibilities with a spectral resolution of $R \approx 30$. HD 169916 was used as the main interferometric and photometric standard star (Procyon in the case of the Orion BN object) and was observed always immediately after the science objects. In addition, all calibrator measurements of a night were collected to create an average interferometric transfer function and to assign error margins to the measured visibilities. We have reduced the interferometric data with the MIA+EWS package, version 1.5, developed at the MPIA Heidelberg and the University of Leiden.

One way to interpret visibilities is to use a combination of simple geometrical configurations like Gaussians, disks, rings, or point sources to construct a synthetic intensity distribution similar to the observed one. Still, to learn more about the potentially more complicated intensity structure, such an ansatz might not always be sufficient. Further, more physically motivated modelling is often necessary for interpretation.

We apply self-consistent continuum radiative transfer modelling in order to produce synthetic MIR intensity maps and to compare their spatial frequency spectrum with the observed visibilities. Here, we are mainly concerned with the question which spatial distribution of the circumstellar material can account for both, the SED and the visibilities of our targets.

We used the SED online fitting tool of Robitaille et al. [19] that can in principle comprise YSO models including an envelope plus circumstellar disk. We refer to this publication for details on the setup of these models. For parameter combinations well fitting the SED, the underlying radiative transfer code of Whitney et al. [25] is then used to produce high-resolution MIR intensity maps for these selected models. Comparing the resulting synthetic visibilities with the observed ones indicates which models finally account for the observed SED *and* visibilities.

3. Results

In this contribution, we concentrate on two objects for which we have reached considerable progress. They show visibilities in the order of 0.2–0.3 at UT baselines. We note that such visibilities, although not reaching the relatively high levels of most Herbig Ae/Be stars [11], are qualitatively different from the very low visibilities (0.01–0.05) found for several of the other objects in our sample as well as recently reported for two other massive YSOs [4, 23].

3.1. M8E-IR: A BN-type object with a bloated central star?

This is a prominent BN-type MYSO at a distance of roughly 1.5 kpc. Although M8E-IR was a well investigated object in the 1980’s, the spatial resolution for most of the IR observations of M8E-IR was poor. An exception is the work by [22] who speculated on the existence of a small circumstellar disk around M8E-IR based on thermal infrared lunar occultation data.

For SED fitting, we use the M8E-IR photometric data collected in [17] plus new 1.2 mm data from [1]. We want to stress that no (sub-)millimeter interferometry on M8E-IR is reported in the literature which could spatially disentangle the flux contributions from M8E-IR and the radio

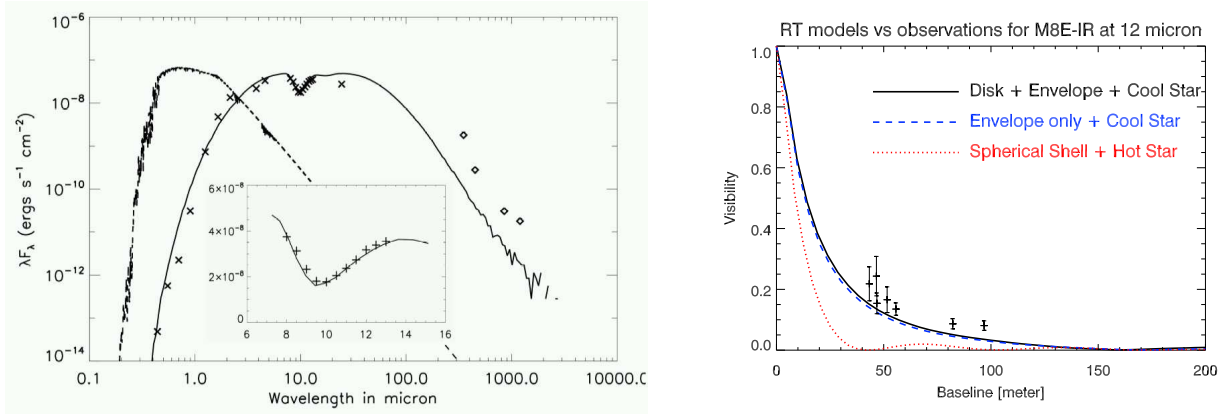


Figure 1. Left: The SED of M8E-IR, shown as crosses (measured fluxes) and diamonds (upper limits). The solid curve denotes the SED of the best-fitting radiative transfer model. The dashed line marks the unreddened SED of the bloated central star for this particular model. The inset is a zoom into the 8–13 micron region that underlines the quality of the fit. **Right:** Comparison of the best-fitting models with bloated cool central star (black solid line and blue dashed line) and a standard configuration including a spherically symmetric shell and a hot central star (red dotted line). Obviously, the latter one is not compatible with the observed visibility data, shown here as plus signs including error bars.

source 8'' away. Hence, we consider the M8E-IR fluxes for $\lambda > 24.5 \mu\text{m}$ just as upper limits in our modelling. Furthermore, we include new optical photometry in the B, V, and I filters reported by [18] as well as our new Subaru 24.5 μm photometry. In addition, the 8–13 μm total flux spectrum taken in the course of the MIDI measurements was used to further constrain the multitude of viable models. We show the SED of the best fitting model in Fig. 1 (Left).

The best-fit model comprises a very compact circumstellar disk (< 50 AU), a larger envelope with small bipolar cavities, and a cool central object ($T_{\text{eff}} \sim 4500$ K). We mention explicitly, that among the well-fitting models there are also configurations without a disk (axisymmetric flattened envelope + outflow cavities only), but also including a cool bloated central star. These nevertheless give almost the same high visibilities. This suggests that in the case of M8E-IR, the choice of the central object might actually govern the resulting visibility levels (see below). Traditionally, such BN-type objects have been modelled as a spherical dust shell surrounding a hot, non-bloated central star [5]. To check if even such canonical configurations can account for the SED and the visibilities we employed well-tested models, based on the code used in [14]. With a purely spherically symmetric geometry and a 24,000 K central star it is possible to find models that reasonably fit the SED of M8E-IR. Still, compared to the measured visibilities, these models result in far too low visibilities (< 0.05) for M8E-IR in the baseline range 30–60 m over the whole 8–13 μm range. The error margins of the MIDI visibilities (on average 10%) do not account for such large differences. In Fig. 1 (Right), as an example the u, v -spectrum of the 12 μm synthetic images based on the cool star models are included as black solid and blue dashed line. They are compared to the corresponding image from the above-mentioned spherically symmetric modelling with hot central star (red dotted line). Although the u, v -spectra of the models with cool central object still show somewhat lower visibilities than the measured ones, obviously they are qualitatively different from the spherically symmetric model with hot central star which fails to match the observational data.

The best-fitting models for M8E-IR in the Robitaille model grid feature central stars of 10–15 M_\odot which are strongly bloated (120–150 R_\odot) and, therefore, have relatively low

effective temperatures. Such solutions can occur since the Robitaille grid comprises the full range of canonical pre-main sequence evolutionary tracks from the Geneva group as possible parametrisation of the central objects. M8E-IR probably cannot straightforwardly be identified with correspondingly very early evolutionary stages, and we refer to [20] for an extensive discussion on the intricate dependencies in the model grid. However, the tendency for a bloated central star in the case of M8E-IR may be valid. As demonstrated already in [9], accretion with high rates onto main sequence stars can temporarily puff up such stars. Further encouragement to consider this comes from recent modelling of the pre-main-sequence evolution of stars in dependence of the accretion rate [6, 26]. These groups find that for accretion rates (onto the forming star) reaching $10^{-3} M_{\odot}/\text{yr}$, the protostellar radius can temporarily increase to $> 100 R_{\odot}$, in accordance with our indirect findings from the model fitting. Interestingly, [15] revealed high-velocity molecular outflows from M8E-IR based on M-band CO absorption spectra and speculated on recent (< 120 yr) FU Ori-type outbursts for this object. If these multiple outflow components really trace recent strong accretion events, the central star could have indeed been affected. In addition, M8E-IR is not detected by cm observations with medium sensitivity [21, 16]. This could be explained by large accretion rates still quenching a forming hypercompact HII region [24]. Furthermore, also a bloated central star with $T_{\text{eff}} \ll 10000$ K would give a natural explanation for these findings.

3.2. The KW Object in M17: An example for the transition towards the Herbig Be star stage

In order to give another example for the abilities of MIR interferometry to assess the viability of different geometric models for a massive YSO, we report here on results for the object M17 IRS1 [2], also called the Kleinman-Wright (KW) Object. We have obtained three visibility measurements with different position angles for UT baselines from 43 m to 56 m. Furthermore, for the first time, we show here MIDI observations towards massive YSOs utilising the 1.8-m ATs. We find clearly different visibility levels for the five measurements, staying at a 0.1–0.3 level for the UT measurement but reaching more than 0.5 for the shorter AT baselines. Also here, we consulted the Robitaille SED fitter in order to find models reproducing the SED. Since the SED of M17 IRS1 is less constrained in the literature than in the case of M8E-IR, the fitter allows for a larger variety of models, all however including an intermediate-sized circumstellar disk and only a very small envelope contribution. In Fig. 2 (Left) we show one example where the 32-m AT measurement is compared to 9 well-fitting models. Here, MIDI can be used as a discriminator. Among the SED-fitting models it rejects very strongly inclined (87°) edge-on models where we see relatively diffuse MIR emission only, since the view onto the central compact disk rim is obstructed by the outer disk. Consequently, such models result in far too low N-band visibilities and do *not* reach the measured elevated visibility levels for any baseline orientation. The less inclined 75° model to the right at least provides a direct view onto the inner hot disk rim and therefore results in clearly higher visibilities than edge-on models.

3.3. Beyond visibilities: Differential phases

For two-element infrared interferometers like MIDI, the *visibility* (and the correlated flux, respectively) is the typical quantity from which further information is derived. To calibrate the absolute position of the fringe phases directly is very difficult in this wavelength regime, and for closure phase measurements at least three beams are necessary. However, it is possible to extract the *differential phase* for the MIDI data within the coherent data reduction algorithm presented in [7]. This quantity can tell us about the geometry of the object under investigation. Point-symmetric objects have a differential phase of zero. Differential phases deviating from this are related to position shifts of the photo-centre over wavelength. This can be considered as an analogon to the signal derived from conventional spectro-astrometry measurements.

In Fig. 3 we show the differential phases for the well-known BN object in the Orion BN/KL

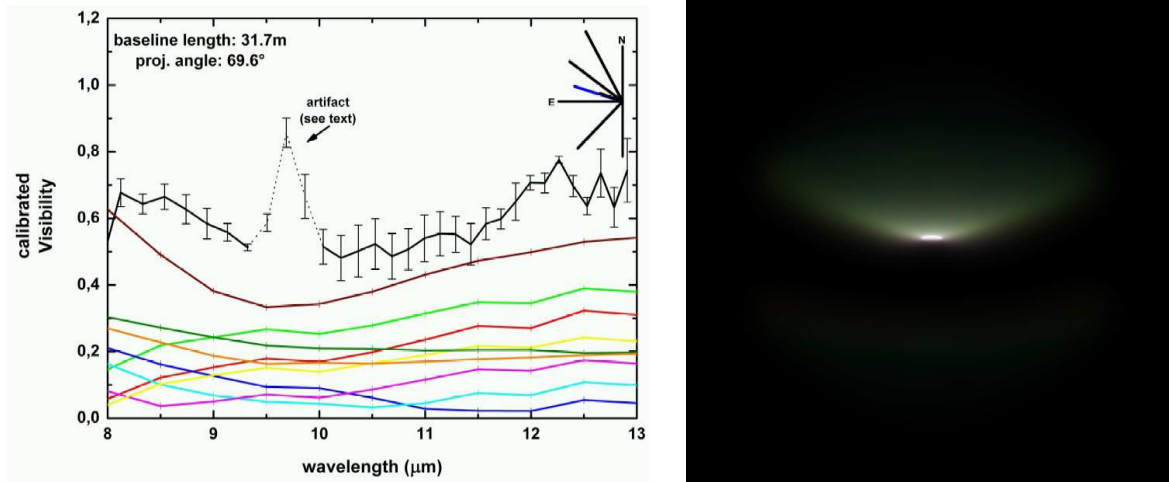


Figure 2. Left: Observed visibility curve (black line with error bars) for the 32-m AT baseline for the KW Object in M17. The coloured lines give cuts through the synthetic MIR maps of different models well fitting the SED. The 75° inclination model (brown curve) clearly stands out as coming closest to the observed visibilities. **Right:** Synthetic $8-13 \mu\text{m}$ image (in logarithmic stretch) for the 75° inclination model delivered by the Robitaille fitter for the KW Object (see left panel). Displayed is a linear size of $1400 \times 1400 \text{ AU}^2$. This model has a disk radius of 500 AU and a $15 M_\odot$ central star with $T_{\text{eff}} = 31000 \text{ K}$. As an important feature, the inner bright disk rim is directly visible which leads to higher visibilities than for most edge-on configurations.

region which we recently observed at several short MIDI baselines with the Auxiliary Telescopes. A significant differential phase signature is obvious. This supports recent claims that Orion BN is deviating from spherical symmetry, reported in [8], where these authors infer the presence of a compact circumstellar disk by means of near-IR polarimetric observations.

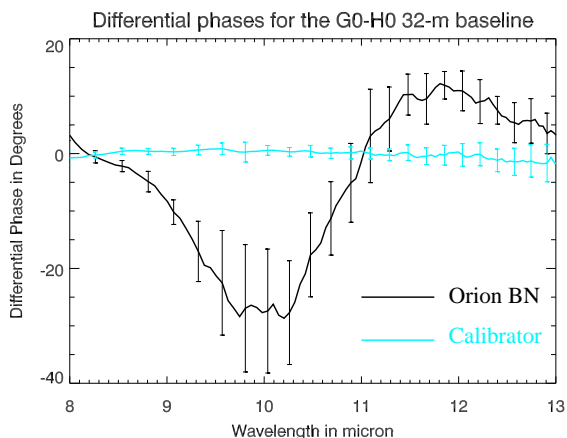


Figure 3. Differential phases for the BN object in Orion. Shown are the data from the 32-m AT baseline, including the $3\text{-}\sigma$ error bars, for BN and the calibrator closest in time to the science object. Under ideal observing conditions, the differential phases for a calibrator ought to be constant at zero degrees. The significant differential phase signal for BN indicates a deviation from spherical symmetry on scales of around 75 milli-arcseconds traced by this baseline.

4. Conclusion

We have observed massive young stellar objects with the MIR interferometer MIDI at the VLTI. We find substructures with MIR sizes around 30–50 mas. Using the measured visibilities as discriminator, we can exclude purely spherically symmetric matter distributions with a hot central star for the object M8E-IR. The most probably configuration consists of a compact circumstellar disk surrounded by a larger envelope plus a cool central object. The total disk size is not well constrained by the models, and the data allow also for an envelope-only configuration. The finding of a cool central object inside this MYSO is consistent with the idea that the 10–15 M_{\odot} central star has been strongly bloated by recent strong accretion events.

For M17 IRS1, we can exclude the nearly edge-on disk models which were among the models suggested by the SED fitting. Instead, a moderately inclined circumstellar disk might be closer to the truth, and the results of a disk-dominated object with small envelope contribution support an earlier suggestion that M17 IRS1 is near to the Herbig Be star phase.

Our results show that IR interferometry is a viable tool to reveal decisive structure information on embedded MYSOs and to resolve ambiguities arising from fitting the spectral energy distribution. With the inclusion of the Auxiliary Telescopes, the VLTI is currently becoming even more flexible to tackle such tasks. Finally, the 2nd-generation VLTI instrument MATISSE [13] for the thermal IR will reveal even more complex details of MYSOs by adding closure phase and imaging capabilities to MIR interferometry.

References

- [1] Beltrán M T, Brand J, Cesaroni R, et al. 2006 *A&A* **447** 221
- [2] Chini R, Hoffmeister V H, Kämpgen K, et al. 2004 *A&A* **427** 849
- [3] De Buizer J M 2006 *ApJL* **642** L57
- [4] de Wit W J, Hoare M G, Oudmaijer R D and Mottram J C 2007 *ApJL* **671** L169
- [5] Henning Th 1990 *Fundamentals of Cosmic Physics* **14** 321
- [6] Hosokawa T and Omukai K 2008 *ApJ (accepted) Preprint* arXiv:0806.4122
- [7] Jaffe W J 2004 *Proc. SPIE* vol **5491** ed W A Traub 715-724
- [8] Jiang Z, Tamura M, Fukagawa M, Hough J, Lucas P, Suto H, Ishii M and Yang J 2005 *Nature* **437** 112-5
- [9] Kippenhahn R and Meyer-Hofmeister E 1977 *A&A* **54** 539
- [10] Leinert C, et al. 2003 *Proc. SPIE* **4838** ed W A Traub 893
- [11] Leinert, C. et al. 2004 *A&A* **423** 537
- [12] Linz H, Stecklum B, Henning T, Hofner P and Brandl B 2005 *A&A* **429** 903
- [13] Lopez B, et al. 2006 *Proc. SPIE* vol **6268** ed J D Monnier et al. 31
- [14] Men'shchikov A B, Henning Th and Fischer O 1999 *ApJ* **519** 257
- [15] Mitchell G F, Allen M, Beer R, et al. 1988 *ApJL* **327** L17
- [16] Molinari S, Brand J, Cesaroni R, Palla F and Palumbo G 1998 *A&A* **336** 339
- [17] Mueller K E, Shirley Y L, Evans II N J and Jacobson H R 2002 *ApJS* **143** 469
- [18] Prisinzano L, Damiani F, Micela G, and Sciortino S 2005 *A&A* **430** 941
- [19] Robitaille T P, Whitney B A, Indebetouw R and Wood K 2007 *ApJS* **169** 328
- [20] Robitaille T P 2008 *ASP Conf. Ser.* Vol **387** ed H Beuther, H Linz and Th Henning 290-5
- [21] Simon M, Cassar L, Felli M, et al. 1984 *ApJ* **278** 170
- [22] Simon M, Peterson D M, Longmore A J, Storey J W V and Tokunaga A T 1985 *ApJ* **298** 328
- [23] Vehoff S, Nürnberger D E A, Hummel C A and Duschl W J 2008 *ASP Conf. Ser.* Vol **387** ed H Beuther, H Linz and Th Henning 444-7
- [24] Walmsley M 1995 in *Rev. Mex. Astron. Astrofis. (Conf. Series)* **1** 137
- [25] Whitney B A, Wood K, Bjorkman J E and Wolff M J 2003 *ApJ* **591** 1049
- [26] Yorke H W and Bodenheimer P 2008 *ASP Conf. Ser.* Vol **387** ed H Beuther, H Linz and Th Henning 189-96